Thermo- and chemical-triggered overhand and reef knots based on liquid crystal gels

Zongdai Liu, Hao Zeng, Kun-Lin Yang, Dan Luo

Zongdai Liu, Dan Luo
Department of Electrical and Electronic Engineering, Southern University of Science and Technology,
Xueyuan Road 1088, Shenzhen, Guangdong,
518055, China.
Email: luod@sustech.edu.cn.

Zongdai Liu, Kun-Lin Yang
Department of Chemical and Biomolecular Engineering, National University of Singapore,
4 Engineering Drive 4,
117585, Singapore.
E-mail: cheyk@nus.edu.sg.

Hao Zeng
Smart Photonic Materials, Faculty of Engineering and Natural Sciences, Tampere University,
P.O. Box 541, 33101 Tampere, Finland.

Keywords: soft actuator, liquid crystal gel, overhand knot, reef knot, thermal responsive, chemical responsive.

Abstract: Knot is worldwide used complication and one of the most ancient technologies in human history. A knot can be found in a wide range of applications such as providing practical structural robustness and mechanical connections between objectives. Here, we report a responsive knot that can self-adjust its geometry upon external stimuli. The knot is tightened in a thread made of a liquid crystal gel, of which diameter and internal friction vary upon thermo/chemical stimulus. An overhand knot and a reef knot are demonstrated to exhibit auto-untie action responsive to external stimuli. A self-dropping device is shown to sense its surrounding temperature and chemical change in the environment, providing the proof-of-concept for sensing application. The results offer new alternatives for soft micro robots and automation control for non-electric devices.

1. Introduction

A knot is a structure by winding a one-dimensional material thread into a complicated architecture, to attain mechanical advantages or decorative purposes. The application of knots accompanies people along the development of the entire human civilization. With a clear evidence, the application of knots can date back to 1700 B.C., where Antonians and Mesopotamians were using knots as a seal sign for exchanging goods.[1] Till today, knot is a popular structure used for attaching, binding and constricting especially in surgery,[2] sailing, mountaineering and weaving. For instance, surgical knots are often applied to binding tissue for accelerating wound healing and avoiding wound tearing.[2b] According to complexity, slipperiness and robustness, different knots including half hitch, square knot and surgeon's knot are chosen for different binding purpose.[3]

For adaption of knots into various applications, people are dedicated to develop technologies upon knots in both scientific and engineering angles. For example, knotting system is invented for continuously, effectively and automatically knotting wig on hair.[4] Easy and simple knotting method is invented to knot glass fiber bundles.[5] Knots were studied mathematically as an example of many circles embedded in three-dimensional Euclidean space.[3, 6] Based on improvements of properties, knots were found to be existed in various materials such as nanocarbon,[7] silica microfiber[8] and polymer.[9] However, all the reported knots are based on passive material thread, once it is tightened, and it required extra effort to reverse the process. A knot capable of untying itself upon certain stimuli signal can provide additional degree of freedom of mechanical control and new alternatives for environmental sensing, which is quite useful for many potential applications. However, such capacity requires inclusion of responsive material in the knot construction.

Responsive materials can reversibly deform their shapes upon external stimuli, and have

attracted great attention recently in the fields such as artificial muscles,[10] wearable electronics,[11] drug delivery[12] and so on. Common smart materials include dielectric elastomers,[13] hydrogel,[14] shape memory polymer[15] and liquid crystal polymer network.[16] Liquid crystal polymer network is able to change its orientation order from liquid crystal state to isotropic state, thus it possesses large deformation responses to external stimuli including light,[17] heat,[18] electricity[19] and chemical.[20] Typically, liquid crystal elastomer (LCE) is consisted of reactive mesogens that have fully crosslinked into polymer network during polymerization. Liquid crystal gel (LCG) is consisted of both crosslinked mesogens and non-crosslinked low-molecular-weight liquid crystals. An outstanding advantage of LCG over LCE is that LCG possesses a lower phase transition temperature because of the co-existence of non-reactive liquid crystals in the polymer network.[21] Moreover, a unique response of LCG to external stimuli is that low-molecular-weight liquid crystal may be secreted out from polymer network, which decreases friction and adhesive force.[22] Therefore, the LCG is considered to be an excellent material to fabricate a mechanically tunable structure, where shape-change and friction coefficient pose significant influences on the mechanical property.

Here, we report a thermo- and chemical-responsive LCG overhand knot and reef knot. By elevating the environmental temperature, the LCG overhand knot increases its stabilized diameter gradually, to untie eventually. The underlying mechanism of the geometry change is discussed in details based on the interaction between elasticity and friction forces, where the temperature-dependent diameter change of LCG thread and a phase-transition-based friction reduction are the key factors for untying the knot geometry. We demonstrate two reef knots with programmable weight dropping ability, by responding to heat and chemical vapor pressure (toluene), respectively. The results are expected to provide a new approach for stimuli control over mechanical property

in soft actuators and micro robotics.

2. Results and discussion.

2.1. Physics of overhand and reef knots.

Figure 1 demonstrates the schematic illustrations of two kinds of knots, the overhand knot and the reef knot, with their force analysis. As shown in Figure 1a, an overhand knot is formed based on an elastic rod with circular cross-section diameter (d), where the tensile forces (T) are applied at the both ends to tie it and leads to an overhand knot with a diameter of D ($D = \frac{D_1+D_2}{2}$). The tensile force (T) to hold the knot and the elastic energy (U) stored inside the knot can be represented by[23]

$$T = \frac{2\mathrm{EI}}{D^2}, \tag{1}$$

$$U = \frac{2\pi\mathrm{EI}}{D}, \tag{2}$$

where E is the Young's modulus and I is moment of inertia.

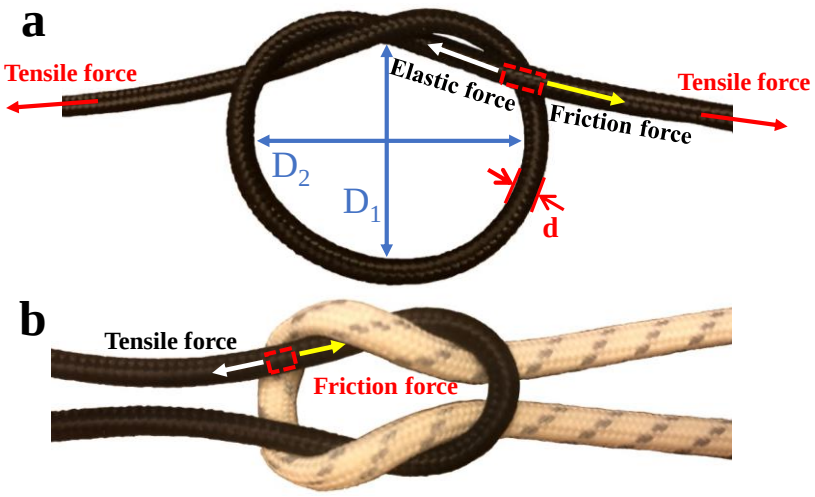

Figure 1. Schematic illustrations of (a) the overhand knot and (b) the reef knot.

When the two ends of a knot are pulled (to tighten the knot) and then released, the elastic energy stored during tightening process trends to be released, pushing the thread backward and

elevating the diameter of knot D. Then, the diameter of knot D will stop to increase while the friction force and elastic force are equal to each other, leading to a stabilized and minimized diameter of knot D_m. At this mechanical equilibrium, the elastic force tends to be restored into the original elastic rod while the friction force at the braided region blocks it. The knot will stay in a static state where the relationship between the friction force and elastic force can be calculated by[23b, 24]

$$\mu = 1.02\sqrt{d/D_m}\,, \tag{3}$$

where μ is the friction coefficient. It is thus known that the geometry of a tightened knot at the mechanical equilibrium is determined by the several physical parameters such as friction coefficient μ, diameter of thread d and minimized knot diameter D_m. A drop of friction coefficient or an increase of thread diameter will lead to an elevation of D_m, which is a sign of untying process.

As shown in Figure 1b, a reef knot formed by two elastic rods is stabilized when the tensile force (T) is balanced by the friction force (f), as

$$T \leq f. \tag{4}$$

If N represents the normal force squeezing two elastic rods, the friction force yields to

$$f = 2\mu N, \tag{5}$$

where the factor 2 represents two contacting spots. Therefore, an equilibrium state yields to

$$T \leq 2\mu N. \tag{6}$$

The normal force N can be further represented by

$$N = Te^{\mu\pi}, \tag{7}$$

when the elastic rod is wrapped around a cylinder along an arc through π radians. Therefore, upon combining Equation (6) and (7), the equation becomes[25]

$$1 \leq 2\mu e^{\mu\pi}. \tag{8}$$

2.2. A thermally responsive LCG overhand knot.

Here, we propose a thermally responsive liquid crystal gel (LCG) overhand knot. To fabricate the overhand knot, a thread is firstly formed based on LCG (**Figure 2**a) by flowing the mixture in a rubber tube. Then a shear stress is applied along the long direction of the thread to induce planar orientation of LCG molecular. Subsequently, ultra-violet (UV) polymerization is applied for stabilizing the entire network. After polymerization, the material undergoes a phase transition upon heating, resulting in an increment of thread diameter, which is one of the key factors for controlling the state of the knot. The schematic configuration and mechanism of the thermal responsive LCG are shown in Figure 2b and 2c, respectively. With the increase of temperature, the thread will become short along the long direction and the diameter of the thread will become larger, as shown in Figure 2b. The reason is demonstrated in Figure 2c. At the beginning, the alignment of liquid crystal molecules is aligned along the long direction of the thread. Upon heating, the liquid crystal molecules change from liquid crystal phase to isotropic phase, leading to a shrink along the long direction of the thread and expansion along the perpendicular direction for a larger diameter.

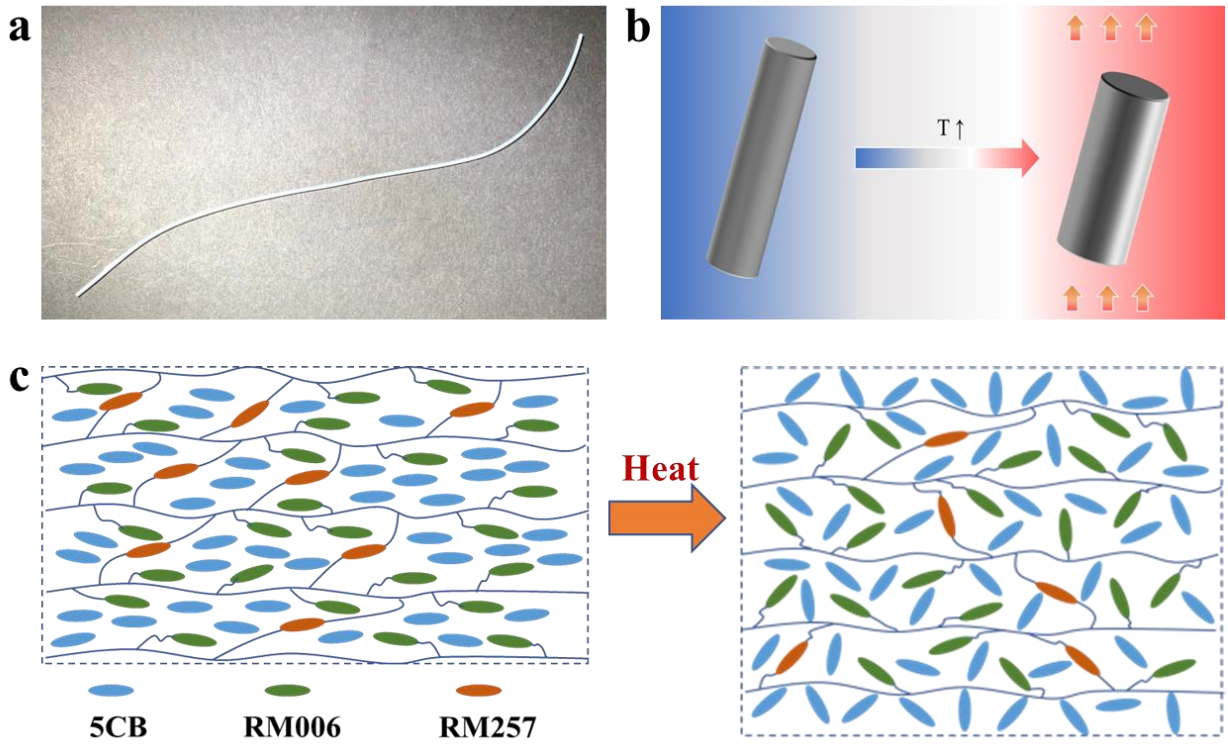

Figure 2. The LCG polymer thread and its response to heat. (a) An LCG polymer thread sample. (b) The schematic configuration of thermal responsive LCG polymer thread upon heating. (c) The change of liquid crystal molecules orientation during heating.

The LCG thread is then manually tied to form an overhand knot (see Methods). The knot is tightly held and then released at the surface of glycerol to reach a mechanically stabilized state at temperature of 22 °C. When the knot is pulled by hand, the tensile force is equal to the sum of friction force and elastic force. Once the tensile force is removed by stopping pulling two ends, the diameter of knot D starts to increase as the elastic force is larger than the friction force. After the elastic force reaches an equilibrium state with friction force, the knot stops to expand and stabilizes, as shown in **Figure 3**a and Video 1. Here, the stabilized diameter of the LCG overhand knot can be calculated by: $D_m = \frac{D_1+D_2}{2} = 17.2$ mm, where D_1 and D_2 are diameters, as shown in Figure 1a. When the temperature is increased, the stabilized diameter of overhand knot becomes larger. Figure 3b shows the photo of the LCG overhand knot at temperature of 80 °C.

When the temperature is at 22 °C and 30 °C, the stabilized diameter of knot is relatively small as 17.2 mm and 17.5 mm, respectively. When the temperature increases to 40 °C, the diameter of knot increases abruptly to 20.5 mm. With a further increased temperature, the diameter of knot increases gradually from 20.6 mm (50 °C) to 24.40 mm (90 °C), and the unknotting of overhand knot completes at temperature of 100 °C (as shown in Figure 3c). Figure 3d plots the relationship of the stabilized diameter of knot D_m and temperature (from 22 °C to 90 °C).

With increase of temperature, the diameter of LCG thread increases linearly. This is because the abrupt phase transition process from liquid crystal state to isotropic state changes into a gradual process. As shown in Figure S1, a peak at 45 °C is observed before polymerization, indicating an abrupt phase transition occurs. After polymerization, no peak is observed while a plateau is observed after 35 °C, indicating a 2nd order phase transition occurs from liquid crystal state to isotropic state.[26] The detailed expansion of the diameter of LCG thread with increased temperature is shown in Figure 3e. An increment of 8.01% expansion rate is obtained when the temperature reaches up to 100 °C. The photos of LCG thread at different temperature are shown in Figure S2.

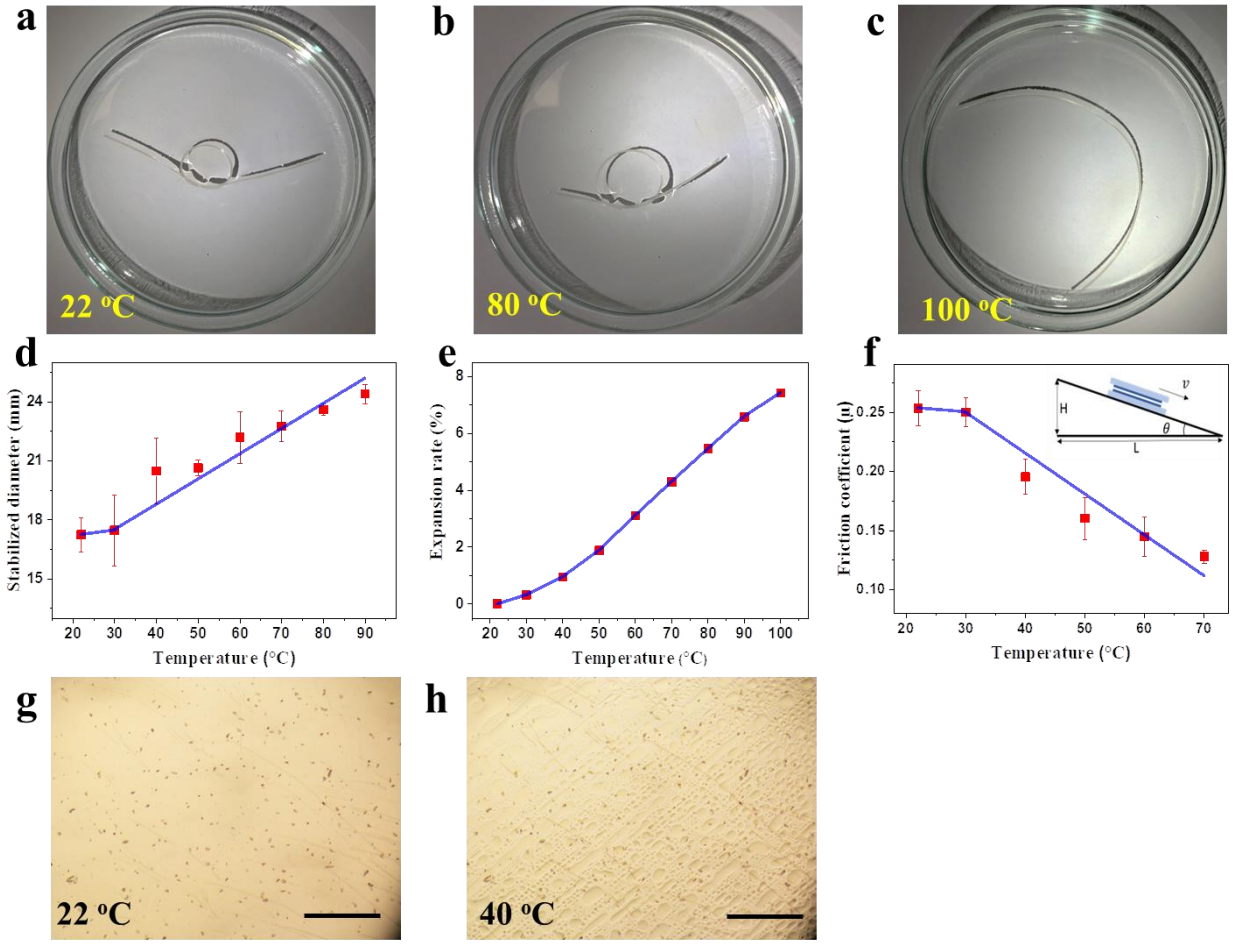

Figure 3. Thermal responsive LCG overhand knot. Photos of the LCG overhand knot at (a) 22 °C, (b) 80 °C, and (c) 100 °C. (d) The relationship of the stabilized diameter of knot D_m and temperature. (e) The expansion rate of diameter of LCG thread versus temperature. (f) The relationship of friction coefficient μ and temperature. The texture of an LCG film under optical microscope at (g) 22 °C and (h) 40 °C. Scale bar: 500 μm.

According to Equation 3, both diameter of LCG thread and the friction coefficient determine the value of the stabilized diameter of knot D_m. Figure 3f plots the relationship of friction coefficient μ and temperature (from 22 °C to 70 °C). The schematic configuration for friction coefficient measurement is shown in the inset of Figure 3f (see Methods). An LCG film is fixed on a slope, while the other film is placed onto it to slide from top to bottom. When the upper film slid down at a constant velocity, the ramping angle is recorded to calculate the friction coefficient. As shown in Figure 3f, a small difference of friction coefficient occurred when the temperature

increases from 22 °C to 30 °C. It is worth noting that an abrupt drop of friction coefficient (from 0.25 to 0.20) occurs at 40 °C. The friction coefficient further decreases to 0.15 as the temperature reaches up to 70 °C. To further study the underlying mechanism of the drop, an LCG film is heated under an optical microscope. When the film is heated from 22 °C to 40 °C, it is clearly to view that several droplets are secreted to the surface of LCG film, as shown in Figure 3g-3h. When the temperature is equal to the clearing temperature of liquid crystal 5CB (35 °C), the volume of liquid crystal 5CB will increase.[27] Simultaneously, the polymer network is turning from planar orientation in liquid crystal phase to isotropic phase, where the volume of voids inside the polymer network will decrease. Therefore, the liquid crystals are no longer able to be caged inside the polymer network and they will be squeezed out from the thread, resulting in a slippery surface with an abrupt drop of friction coefficient at 40 °C. With a further increased temperature, the droplets secrete more and more (as shown in Figure S3). Therefore, the friction coefficient drops further.

2.3. Thermally responsive LCG reef knot.

Two LCG threads are firstly manually tied to form a reef knot, as shown in **Figure 4**a. Then the knot is tapped and held vertically in the air with a weight (1 gram to 5 grams) attached to it (Figure 4b). The reef knot hanged with a weight is then placed inside an oven to be heated up. For the case that 1 gram weight is hanged, the reef knot stays static at beginning. When the temperature reaches the critical temperature of 43.5 °C, the thread at the lower part starts to slide and fell down abruptly (Figure 4c). Here, the reef knot is separated to two independent parts where the upper part is a U shape and the bottom part is fallen down the ground with the weight. When the temperature is above the clearing point of LCs 5CB (35 °C), the LCs emerge at the surface of LCG thread,

resulting in a decreased friction force. Moreover, the diameter of LCG thread increases gradually with increased temperature (Figure 3e), leading to the falling down of the bottom part of thread.

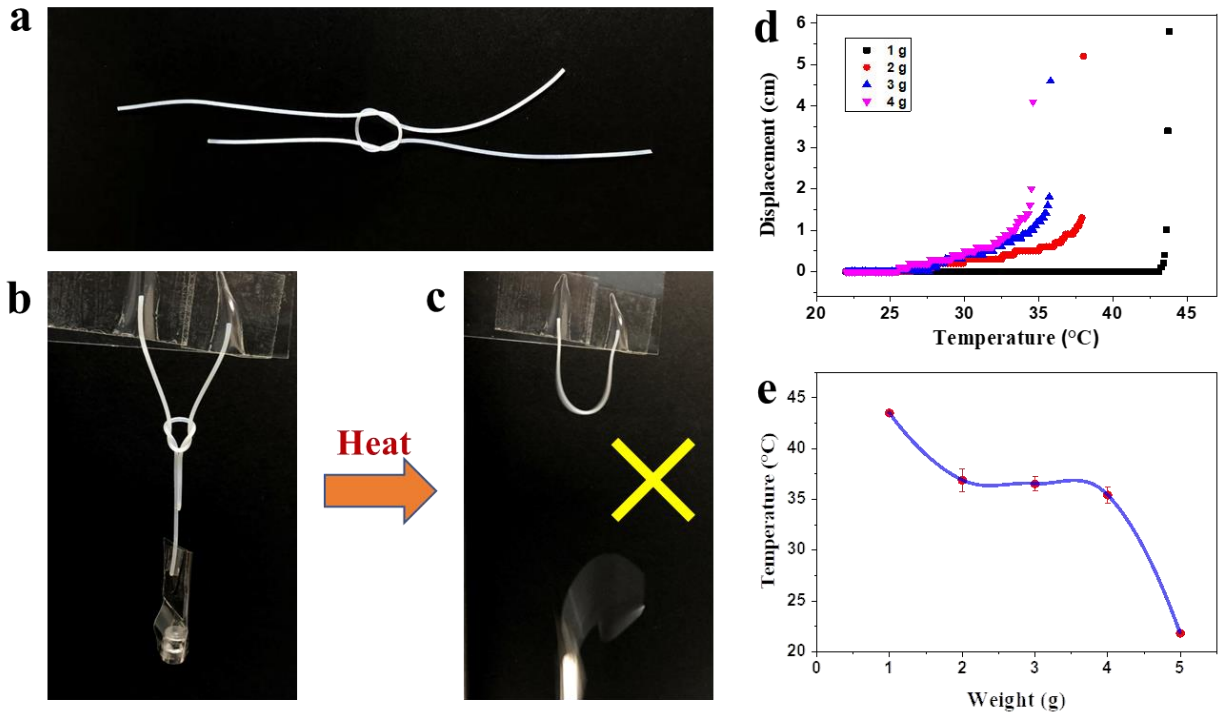

Figure 4. Thermal responsive LCG reef knot. (a) Photo of LCG reef knot at free. (b) Photo of LCG reef knot hanging with a weight of 1 gram. (c) Photo of LCG reef knot at status of falling down at temperature of 43.5 °C. (d) The displacement of the weight hanging on the reef knot versus the temperature. (e) The critical temperature for falling down of reef knot versus hanging weight.

In our experiment, the critical temperatures for reef knot with hanging weights of 2 grams and 3 grams are observed to be 36.9 °C and 36.5 °C, respectively, which are both above the clearing point of 5CB (35 °C). The critical temperature for reef knot with hanging weight of 4 grams is 35.4 °C, which is also around the clearing point of 5CB. Figure 4d plots the displacement of the weight versus temperature with different hanging weights (1 gram to 4 grams). In the beginning, the weight is at static and the displacement was zero. When the weight falls down from reef knot, the displacement abruptly reaches maximum. The critical temperature for falling down of reef knot versus hanging weight is demonstrated in Figure 4e. For reef knot with hanging larger weights

such as 5 grams, the reef knot is separated into two parts at room temperature (22 °C), which indicates that the carrying limit weight of our reef knot.

2.4. Chemical-responsive LCG overhand knot.

Besides thermo, liquid crystal polymers can react to volatile organic compounds, generally by swelling.[28] In our experiment, toluene is used to trigger the unknotting process of the LCG overhand knot. **Figure 5**a shows the unknotting process of the LCG overhand knot immersed in toluene isopropanol solution with different toluene concentrations of 0% (v/v) (Figure 5a-i), 20% (Figure 5a-ii), 40% (Figure 5a-iii) and 60% (Figure 5a-iv). When the concentration of toluene is 0%, the diameter of the overhand knot in the solution is measured to be 10.9 mm. With an increased toluene concentration, the stabilized diameter increases from 14.0 mm (20%) to 25.0 mm (40%). Finally, when the toluene concentration reaches 60%, the knot is unknotted in the solution of toluene.

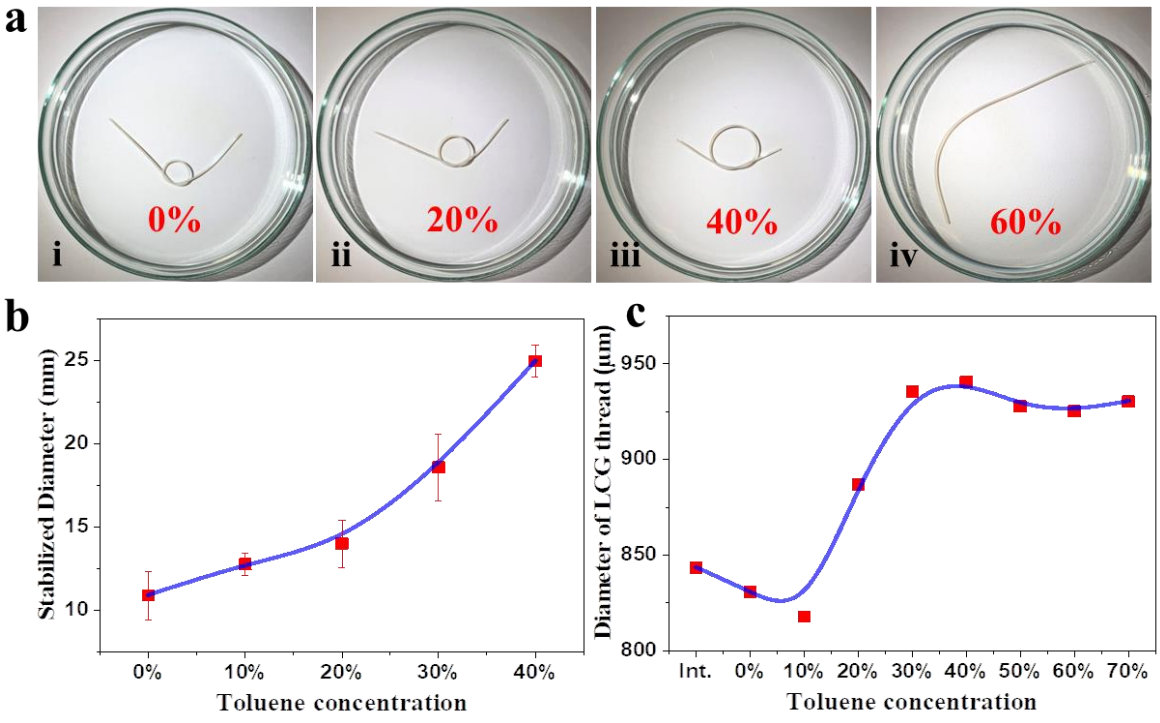

Figure 5. Response of overhand knot to toluene. (a) Toluene-responsive overhand knot and reef knot. (a) The diameter of the knot increased with increased toluene concentration from 0% (v/v) to 60% in isopropanol solution. At a concentration of 60%, the overhand knot was unknotted into a thread. (b) The stabilized diameter of the knot increased with increased toluene concentration. (c) The diameter of LCG thread decreased first and then increased with increased toluene concentration.

The trend of the stabilized diameter (D_m) versus toluene concentration is shown in Figure 5b. The stabilized diameter of overhand knot is 10.9 mm, 12.8 mm, 14.0 mm, 18.6 mm, and 25.0 mm when the toluene concentration is 0%, 10%, 20%, 30% and 40%, respectively. When the toluene concentration is beyond 50%, the knot no longer exists. The change of stabilized diameter of the overhand knot can be influenced by two factors including the diameter of the thread and the slipperiness of the thread. Figure 5c and Figure S4 shows the relationship of diameter of LCG thread and toluene concentration. The initial diameter of LCG thread is 843.4 mm. When the LCG thread is fully immersed into isopropanol, the diameter of the LCG thread decreases to 830.7 mm and further decreases to 817.9 mm when the toluene concentration increases to 10%, which is because that the volume of unpolymerized 5CB in LCG increases when it transits to isotropic state as isopropanol or toluene is absorbed by the 5CB. With further increase toluene concentration, the room of original micropores in the polymer network is no longer sufficient to contain the enlarged 5CB, resulting in the excretion of 5CB from the polymer network. Therefore, the LCG slightly collapses and the diameter of LCG thread decreases when the concentration of toluene increases from 0% to 10%. With a further increased concentration of toluene above 10%, the toluene is then absorbed by the polymer network, resulting in a further increased diameter of LCG thread. However, the diameter of the LCG thread reaches a saturated value around 930.0 mm when the toluene concentration reaches 30%.

2.5. Chemical-responsive LCG reef knot.

Similar to the case of thermal responsive LCG, when the LCG is exposed to toluene vapor, the LC 5CB will secrete from the surface of LCG film, leading to unknotting of LCG reef knot. The photo image of the LCG film without toluene vapor is shown in Figure S5a. With exposed to a saturation concentration (37,000 ppm at 25 °C) toluene vapor, the LCG film starts to wrinkle as the secrete of 5CB on the surface of LCG thread, and the friction force between two threads is decreased as well, leading to the increase of stabilized diameter of the knot (Figure S5b).

In our experiment, a LCG reef knot is fabricated to measure the toluene vapor responsiveness. A circuit composed by a power supply, a switch and a light emitting diode (LED) is designed for alerting toluene vapor leakage, as shown in **Figure 6**a. The switch is consisted of two conductive tapes and a conductive weight, as shown in Figure 6b and Figure S6. The two conductive tapes with a small gap are adhered on the glass substrate, and the weight is hanged by the LCG reef knot. The switch is controlled by the location of a conductive weight. When the weight is hanging by the reef knot, the switch is off and the circuit is open (Figure 6c). When the weight falls down from the LCG reef knot in toluene vapor with a saturated concentration (37,000 ppm), it contacts with the conductive tapes and the electric circuit is activated (LED on, Figure 6d). This LED light signal enables an alert of toluene leakage when it is exposed to saturated toluene vapor.

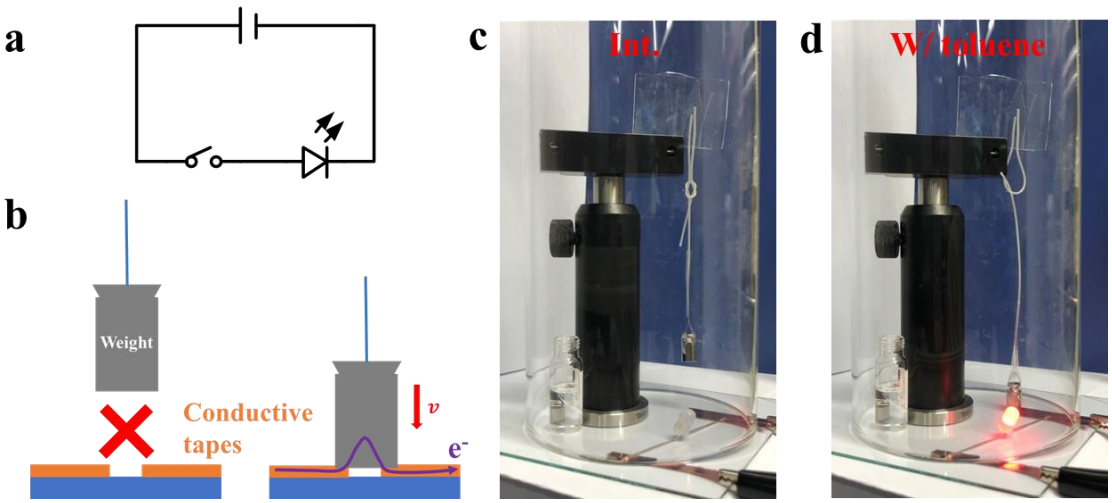

Figure 6. Toluene vapor responsive LCG reef knot. (a) The electrical circuit. (b) Schematic illustration of connection of the electric circuit. (c) Initial state of toluene vapor responsive LCG reef knot. (d) Within toluene vapor, the weight on the LCG reef knot drops and lights LED on.

3. Conclusion.

In conclusion, we fabricate overhand knot and reef knot that are able to be unknotted automatically by increasing temperature. Upon increasing temperature of LCG threads, the slipperiness of LCG thread surface increases, resulting in the decrease of friction coefficient. Moreover, the diameter of LCG thread becomes larger with increased temperature. Therefore, the diameter of overhand knot increases and the weight of reef knot fall down. Interestingly, toluene is applied as well for the same effect. Planar oriented liquid crystalline molecules change their orientation into disordered when exposed to toluene. Therefore, the diameter of the LCG thread increases and the slipperiness increases, which result in the increased diameter of overhand knot in toluene solution. Moreover, toluene vapor is further used to activate the falling down of a weight on a reef knot, which enables a possibility of autonomous control with no power supply.

4. Methods.

Fabrication of LCG thread: The liquid crystal gel (LCG) thread is made by the polymerization of

a mixture of 39.5% (w/w) monomer RM006 (Sdyano, China), 10% crosslinker RM257 (HCCH, China), 50% non-reactive liquid crystal 4-cyano-4'-pentylbiphenyl (5CB) (HCCH, China) and 0.5% photo-initiator Irgacure 819 (Sigma-Aldrich). The mixture is filled inside a syringe which is connected to a rubber tubing with a diameter of 0.8 mm. A syringe pump is applied to drive the flow of the mixture in the rubber tubing. The orientation of liquid crystalline mixture is controlled by the flow rate which was adjusted by the syringe pump. With the volumetric flow rate of 1 L min^{-1}, the mixture is polymerized under UV light. The intensity of UV light is measured to be 15.1 W cm^{-2} (FieldMaxII, Coherent, the USA). After 15 s of UV exposure, the movement of the mixture stops and the orientation of the liquid crystalline mixture is stabilized by the formation of LCG. The polymerized LCG thread is pulled out from one end of the rubber tubing by applying a pressure at another end.

Manually fabricated knots: The processes to fabricate an overhand knot and a reef knot are shown in Figure S7. To form an overhand knot (Figure S7a), a LCG thread is firstly used to form a loop. Then one end of the thread is tucked into the loop. Finally, the two ends of knot are hold and pulled into tight. The reef knot (Figure S7b) is formed based on two LCG threads. One thread is formed as U shape and fixed. Another thread is crossed over, and tucked out from the loop. Finally, the four ends of two threads are held and tightened to form the reef knot.

Thermal-responsive unknotting process of overhand knot: A manually-tied overhand knot is placed at the top surface of glycerol with a temperature from 22 °C to 90 °C. The knot is floating at the top of glycerol due to surface tension. The responsive time of unknotting process is around 30 seconds. The overhand knot is initially tied tightly by applying tensile force at two ends. When the knot is placed at the top of glycerol, the tensile force will release, and the diameter of the overhand knot starts to increase.

Thermal-responsive unknotting process of reef knot: Two ends in the upper part of a reef knot are fixed by tape on a glass slide. One end of the lower part is tangling, and another one is connected to a weight. The whole system is placed inside an oven. After the knot stay still in the oven, the oven is heated. The temperature of the oven increases from 22 °C to 60 °C with a ramp of 2 °C / min.

Measurement of thermal expansion: To clearly distinguish the LCG thread under bright field microscope, 1% (w/w) dye disperse red (Sigma-Aldrich) is doped in the mixture. A piece of LCG thread is cut by a knife. Then the sample is placed under microscope and heated from room temperature (22 °C) to 100 °C. The diameter of LCG thread is measured at every 10 °C.

Measurement of friction coefficient: An LCG film is fabricated in a LC cell with a cell gap of 45 μm. Two glass slides with planar orientation by rubbing polyimide are used to fabricate the LC cell. The same mixture is injected into two cells to form two films. Then the two cells are opened manually. Later on, the two films are contacted each other. One edge of the film is lifted while another edge remains the original state, as shown in Figure 3f. Therefore, the friction is calculated to be $f = gsin\theta = g\frac{H}{\sqrt{H^2+L^2}}$, where g is the gravity, θ is the lifted angle, H is the height of the sample and L is the length. Moreover, the friction coefficient is $\mu = cos\theta$.

Supporting Information

Supporting Information is available from the Wiley Online Library or from the author.

Acknowledgments:

Author contributions: D. L. and K. -L. Y. supervised the project; H. Z. conceived the idea; H. Z. and Z. L. designed the experiments; Z. L. performed the experiments; Z. L. drafted the manuscript; all dedicated to the current version of manuscript.

Competing financial interests: The authors declare no competing financial interests.

Reference

[1] a) J. H. Przytycki, *arXiv preprint math/0703096* **2007**; b) S. Jablan, L. Radović, R. Sazdanović, A. Zeković, *Symmetry* **2012**, 4, 302.

[2] a) J. J. Hage, *World journal of surgery* **2008**, 32, 648; b) C. Zhao, C.-C. Hsu, T. Moriya, A. R. Thoreson, S. S. Cha, S. L. Moran, K.-N. An, P. C. Amadio, *The Journal of bone and joint surgery. American volume* **2013**, 95, 1020.

[3] R. H. Crowell, R. H. Fox, *Introduction to knot theory*, Springer Science & Business Media, **2012**.

[4] I. P. Hong, Google Patents, 2019.

[5] a) S. Jiansong, P. Haijian, Google Patents, 2019; b) S. Jiansong, P. Haijian, Google Patents, 2020.

[6] W. R. Lickorish, *An introduction to knot theory*, Springer Science & Business Media, **2012**.

[7] Y. Segawa, M. Kuwayama, Y. Hijikata, M. Fushimi, T. Nishihara, J. Pirillo, J. Shirasaki, N. Kubota, K. Itami, *Science* **2019**, 365, 272.

[8] a) Y. Wu, Y.-J. Rao, Y.-h. Chen, Y. Gong, *Optics express* **2009**, 17, 18142; b) Y. Wu, T. Zhang, Y. Rao, Y. Gong, *Sensors and Actuators B: Chemical* **2011**, 155, 258; c) X. Jiang, Q. Yang, G. Vienne, Y. Li, L. Tong, J. Zhang, L. Hu, *Applied physics letters* **2006**, 89, 143513.

[9] P. B. Warren, R. C. Ball, R. E. Goldstein, *Phys Rev Lett* **2018**, 120, 158001.

[10] S. M. Mirvakili, I. W. Hunter, *Advanced Materials* **2018**, 30, 1704407.

[11] D. P. Dubal, N. R. Chodankar, D.-H. Kim, P. Gomez-Romero, *Chemical Society Reviews* **2018**, 47, 2065.

[12] D. Schmaljohann, *Advanced drug delivery reviews* **2006**, 58, 1655.

[13] Y. Zhao, L.-J. Yin, S.-L. Zhong, J.-W. Zha, Z.-M. Dang, *IET Nanodielectrics* **2020**, 3, 99.

[14] M. Mahinroosta, Z. J. Farsangi, A. Allahverdi, Z. Shakoori, *Materials today chemistry* **2018**, 8, 42.

[15] T. Liu, T. Zhou, Y. Yao, F. Zhang, L. Liu, Y. Liu, J. Leng, *Composites Part A: Applied Science and Manufacturing* **2017**, 100, 20.

[16] a) P. Xie, R. Zhang, *Journal of Materials Chemistry* **2005**, 15; b) T. J. White, D. J. Broer, *Nat Mater* **2015**, 14, 1087; c) R. S. Kularatne, H. Kim, J. M. Boothby, T. H. Ware, *Journal of Polymer Science Part B: Polymer Physics* **2017**, 55, 395.

[17] a) O. M. Wani, H. Zeng, A. Priimagi, *Nat Commun* **2017**, 8, 15546; b) C. Sánchez-Somolinos, *Liquid Crystalline Polymers* **2020**, 447; c) M. Pilz da Cunha, M. G. Debije, A. Schenning, *Chem Soc Rev* **2020**, 49, 6568; d) M. Wang, B.-P. Lin, H. Yang, *Nature communications* **2016**, 7, 1; e) H. Tian, Z. Wang, Y. Chen, J. Shao, T. Gao, S. Cai, *ACS applied materials & interfaces* **2018**, 10, 8307; f) Z.-Z. Nie, B. Zuo, M. Wang, S. Huang, X.-M. Chen, Z.-Y. Liu, H. Yang, *Nature Communications* **2021**, 12, 1.

[18] a) H. Shahsavan, S. M. Salili, A. Jakli, B. Zhao, *Adv Mater* **2015**, 27, 6828; b) H. Doi, K. Urayama, *Soft Matter* **2017**, 13, 4341; c) H. Xing, J. Li, Y. Shi, J. Guo, J. Wei, *ACS applied materials & interfaces* **2016**, 8, 9440.

[19] a) M. Wang, Z.-W. Cheng, B. Zuo, X.-M. Chen, S. Huang, H. Yang, *ACS Macro Letters* **2020**, 9, 860; b) H. Kim, J. A. Lee, C. P. Ambulo, H. B. Lee, S. H. Kim, V. V. Naik, C. S. Haines, A. E. Aliev, R. Ovalle‐Robles, R. H. Baughman, *Advanced Functional Materials* **2019**, 29, 1905063.

[20] a) T. H. Ware, M. E. McConney, J. J. Wie, V. P. Tondiglia, T. J. White, *Science* **2015**, 347, 982; b) T. Kamal, S. Y. Park, *Chem Commun (Camb)* **2014**, 50, 2030; c) T. Kamal, S. Y.

Park, *ACS Appl Mater Interfaces* **2014**, 6, 18048; d) J. M. Boothby, H. Kim, T. H. Ware, *Sensors and Actuators B: Chemical* **2017**, 240, 511.
[21] H. Shahsavan, A. Aghakhani, H. Zeng, Y. Guo, Z. S. Davidson, A. Priimagi, M. Sitti, *Proc Natl Acad Sci U S A* **2020**, 117, 5125.
[22] a) A. H. Gelebart, D. Liu, D. J. Mulder, K. H. J. Leunissen, J. van Gerven, A. P. H. J. Schenning, D. J. Broer, *Advanced Functional Materials* **2018**, 28; b) Y. Zhan, G. Zhou, B. A. G. Lamers, F. L. L. Visschers, M. Hendrix, D. J. Broer, D. Liu, *Matter* **2020**, 3, 782.
[23] a) V. P. Patil, J. D. Sandt, M. Kolle, J. Dunkel, *Science* **2020**, 367, 71; b) B. Audoly, N. Clauvelin, S. Neukirch, *Phys Rev Lett* **2007**, 99, 164301; c) M. K. Jawed, P. Dieleman, B. Audoly, P. M. Reis, *Phys Rev Lett* **2015**, 115, 118302.
[24] N. R. Chevalier, *Colloids Surf B Biointerfaces* **2017**, 159, 924.
[25] J. H. Maddocks, J. B. Keller, *SIAM Journal on Applied Mathematics* **1987**, 47, 1185.
[26] a) C. McGinty, R. Reich, H. Clark, P. Bos, *Journal of Applied Physics* **2020**, 127; b) Z. Liu, D. Luo, K. L. Yang, *Lab Chip* **2020**, 20, 1687.
[27] R. N. V. Ranga Reddy, A. Suryanarayana, V. R. Murthy, *Crystal Research and Technology* **1999**, 34, 1299.
[28] a) A. Karausta, E. Bukusoglu, *ACS Appl Mater Interfaces* **2018**, 10, 33484; b) B. Drapp, D. Pauluth, J. Krause, G. Gauglitz, *Fresenius' journal of analytical chemistry* **1999**, 364, 121.